

# Journal of Materials and Environmental Science

- Instructions
- Volume 4, N°1, 2013
- Volume 3, 2012
- Volume 2, S1, 2011
- Volume 2, N°4, 2011
- Volume 1, S1, 2010
- Volume 1, 2010



Journal of Materials and Environmental Science is a tri-monthly Journal published.



## Content Vol.7 N9, 2016 pp. 3068-3488

Bioinspired eco-friendly synthesis of ZrO<sub>2</sub> nanoparticles, Uddin I., Ahmad A., J. Mater. Environ. Sci. 7 (9) (2016) 3068-3075

Structural and Temperature-dependent vibrational analyses of the non-centrosymmetric ZnMoO<sub>4</sub> molybdate, Ait ahsaine H., Zbair M., Ezahri M., Benlhachemi A., Bakiz B., Guinneton F., Gavarrri J-R., J. Mater. Environ. Sci. 7 (9) (2016) 3076-3083

Réponse à la salinité de quelques paramètres physiologiques et biochimiques du Blé (*Triticum aestivum* L.) au stade montaison. [Physiological and Biochemical Responses to Salt Stress in Wheat (*Triticum aestivum* L.) at the elongation stage], Ouhaddach M., ElYacoubi H., Douaik A., Hmouni D., Rochdi A., J. Mater. Environ. Sci. 7 (9) (2016) 3084-3099

Synthesis, characterization and biological activities of cis-trans complexes [M(phen)(caf)<sub>2</sub>X<sub>2</sub>] M = Co(II), Fe(II), Mn(II), Cu(II); X: SCN<sup>-</sup>, CN<sup>-</sup>; caf : caffeine; phen : (1,10)phenanthroline, EL Hamdani H., EL Amane M., Atmani Z., Haddad M., J. Mater. Environ. Sci. 7 (9) (2016) 3100-3109

Chemical composition and antibacterial activity of three essential oils from south of Morocco. (*Thymus saturooides*, *Thymus vulgaris* and *Chamaelum nobilis*), El Hattabi L., Talbaoui A., Amzazi S., Bakri Y., Harhar H., Costa J., Desjobert J. M., Tabyaoui M., J. Mater. Environ. Sci. 7 (9) (2016) 3110-3117

UAE *Scrophularia Arguta* (Malisah) Extract as a Corrosion Inhibitor for Mild Steel in HCl Solution, Nahlé A., J. Mater. Environ. Sci. 7 (9) (2016) 3118-3124

Valorization of Traditional Olive Mill Wastewaters as Culture Medium for Microalgae, Slimani Alaoui N., Jbari N., Stitou M., El Yousfi F., El Laghdach A., J. Mater. Environ. Sci. 7 (9) (2016) 3125-3132

Effect of solution flow rate on growth and characterization of nanostructured ZnO thin films deposited using spray pyrolysis, Zargou S., Chabane Sari S.M., Senoudi A.R., Aida M., Attaf N., Hakem I.F., J. Mater. Environ. Sci. 7 (9) (2016) 3133-3147

Experimental Study Of The Determination Of E-pH Diagram For 304SS On A Solution With The Addition Of Bee Wax Propolis Inhibitor, Gapsari F., Soenoko R., Suprpto A., Suprpto W., J. Mater. Environ. Sci. 7 (9) (2016) 3148-3153



## Experimental Study Of The Determination Of E-pH Diagram For 304SS On A Solution With The Addition Of Bee Wax Propolis Inhibitor

F. Gapsari<sup>1</sup>, R. Soenoko<sup>2</sup>, A. Suprpto<sup>3</sup>, W. Suprpto<sup>4</sup>

<sup>1,2,3,4</sup> Department of Mechanical Engineering, Faculty of Engineering, Brawijaya University, Indonesia

Received 06 May 2016, Revised 05 Jul 2016, Accepted 12 Jul 2016

\*Corresponding author. E-mail: [memi\\_kencrut@ub.ac.id](mailto:memi_kencrut@ub.ac.id) ; Tel: (+6281803610855)

### Abstract

The impact of the inhibitor addition in the form of BWP extract in the corrosive environment was reviewed on the E-pH diagram of 304SS. This steel has a main constituent element such as Fe (iron), Cr (chromium) and Ni. Based on the E-pH diagram of Cr and Ni, it is known that the steel is corrosion resistant, as it will form a passivation layer as a protection from corrosion. E-pH diagram is generally constructed with complex thermodynamic calculations or using a certain software. In this research, the construction of E-pH diagram based on experimental results was conducted. The environment control by using an inhibitor is the one by modifying the environment. This study is a continuation of early research on the characteristics of the extract BWP as a corrosion inhibitor. The addition of inhibitor will change the E-pH diagram of 304SS. The research was conducted by potentiodynamic testing. Scan rate used was amounted to 0.001 V / s. The result indicates the presence of E-pH diagram changes with the addition of BWP inhibitor. This study also characterized the thin film surface with atomic force microscopy (AFM).

*Keywords:* AFM, corrosion, diagram E-pH, inhibitor, 304SS.

### Introduction

Inhibitor is generally used to reduce corrosive attack on all that is made of metal [1-2]. The use of inhibitors to overcome the problem of corrosion in acidic environments has been widely studied [3-6]. Inhibitors can reduce and prevent the reaction of the metal with the environment in very small amounts [6-8]. Previous research suggests that inhibitor of bee wax propolis (BWP) has the ability to inhibit the rate of corrosion with physisorption. The optimum concentration of extract adding of BWP at 2000 ppm is determined based on the type of mixed polarization and physisorption [9]. Therefore, this study used BWP as the inhibitor that was added in the environment. The chemical structure of BWP was quercetin. The impact of the inhibitor addition in the form of BWP extract in the corrosive environment was reviewed on the E-pH diagram of 304SS. This steel has a main constituent element such as Fe (iron), Cr (chromium) and Ni. Based on the E-pH diagram of Cr and Ni, it is known that the steel is corrosion resistant, as it will form a passivation layer as a protection from corrosion [10]. During corrosion, some soluble metal phase, the surface of the metal or alloy damaged and some form secondary solid phase at the solid-liquid interface (such as oxides, hydroxides, silicates, sulfides, sulfates, carbonates, nitrates, phosphates, borates, or halides). This diagram is formed by the electrochemical reaction when it reaches equilibrium condition [11-14]. The addition of the inhibitor in the test solutions is expected to change the corrosion conditions shown in the E-pH diagram.

There are still some limitations of E-pH diagram construction for corrosion based on thermodynamic calculations. First, the diagram is plotted based on the thermodynamic equilibrium, not on a realistic and non-equilibrium condition [15-17]. Second, most of the diagrams are presented for pure metal, simple alloy compositions in pure water, or simple solution [15,17]. Third, the pH value in the diagram is not based on the pH of the solution, but of local value in cracks or corrosion products, etc. [15]. Fourth, the protection of metal on passive area depends on the level of perfection of the passive layer so that it cannot be confirmed with the diagram [18].

As the E-pH diagram was constructed on an electrochemical reaction equilibrium condition, an alternative method in order to more easily create E-pH diagram is necessary. Special treatment to determine the effect of the inhibitor in this study was by using optimal concentrations in the test solutions with varying pH. Optimal concentration was obtained after testing BWP extract with concentration variation in the test solutions in previous study [9]. Experiment and manufacture of E-pH diagram of the SS 304 without inhibitor was completed early. Then it was compared to the E-pH diagram with the addition of BWP extract. Manufacture reference of E-pH diagram and changing in the active-passive area in this study is the change in the value of  $E_{corr}$  (corrosion potential) and  $E_p$  (passive potential) in the test solution either without or with inhibitor.

## 2. Materials and methods

### 2.1. Materials and test solutions

The chemical composition of the SS 304 (in % by weight) used was 0.04% C, 0.52 % Si, 0.92% Mn, 0.030% P, 0.002% S, 9.58% Ni, 18.15% Cr, Bal. Fe. SS 304 known density is 7.9 g / cm<sup>3</sup> and the specimen measuring 10 mm x 10 mm x 10 mm was prepared for the working electrode (WE). WE was added to the epoxy resin with a geometric surface area measuring 1 cm<sup>2</sup> and connected / close to (exposed) electrolyte. Prior to testing, the specimen surface was smoothed with sandpaper graded from 400 to 2000, alternately.

Bee wax propolis used is a beehive waste whose honey had been squeezed for 3-4 times. This waste is usually in the form of wax and the remaining honey still attached. Bee wax propolis was extracted by using liquid-liquid method to obtain the optimum conditions. Bee wax propolis extract obtained was characterized by Fourier Transform Infrared Spectroscopy (FTIR) and High Performance Liquid Chromatography (HPLC) [9].

The solution for the manufacture of E-pH diagram without the inhibitor of SS 304 in sulfuric acid is then added with NaOH to obtain the desired pH. Test solutions with various pH 30 solution are pH 0,1,2,3,4,5,6,7,8,9,10,11,12,13,14. The solution with the same pH was also added with BWP inhibitor at 2000 ppm corresponding with the optimum results in previous study [9].

### 2.2. Electrochemical Measurement

The reference used in this test is the Standard ASTM (American Standard and Testing) G-31 [19]. Tests were performed using an electrochemical Autolab PGSTAT128N. Specimens having been prepared were assembled into an electrochemical cell with a Ag / AgCl (3 M KCl) as a reference electrode and a platinum as an auxiliary electrode. Those three electrodes were immersed in a batch for 30 minutes. Measurement of polarization in the changes -1 V to +1 V was along the corrosion potential (OCP) with a scan rate of 0001 V / s. The determination of active, passive, and transpassive points was shown in Figure 1.

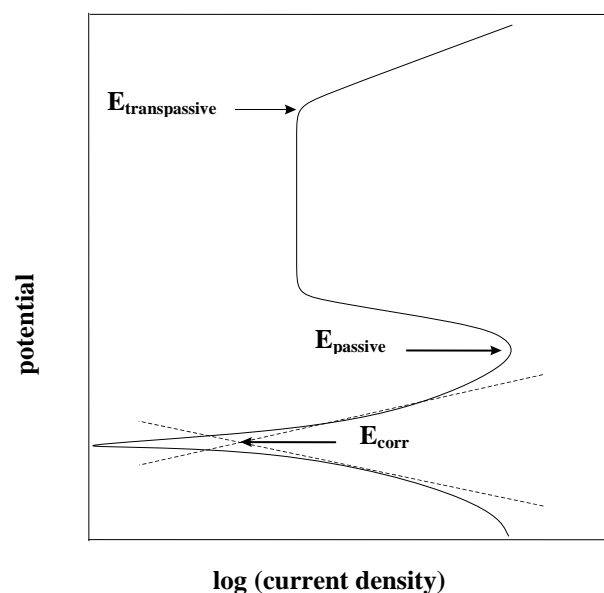
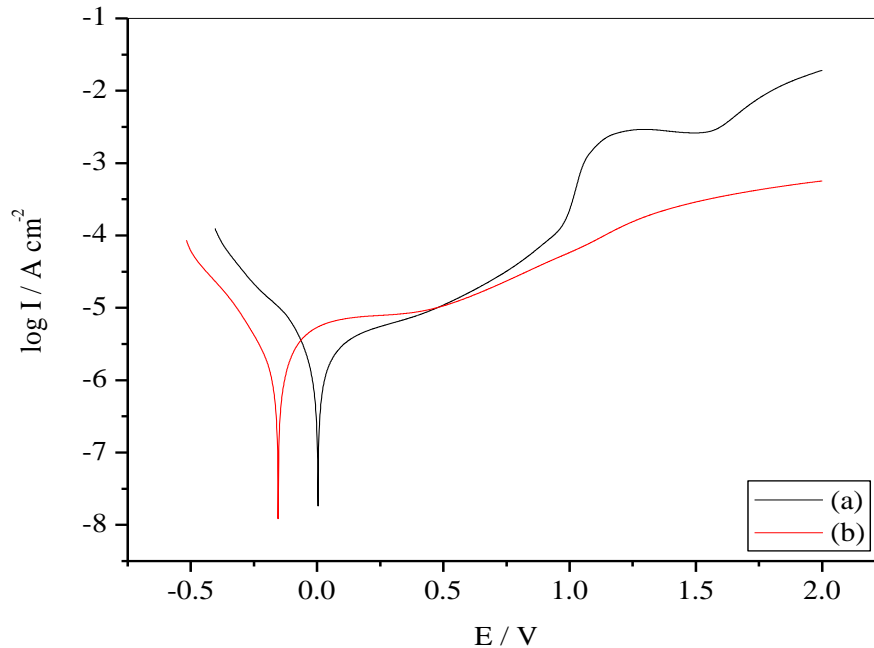


Figure 1: The determination point of  $E_{corr}$ ,  $E_{passive}$ , dan  $E_{transpassive}$

Figure 1 shows the typical curve potentiodynamic anodic polarization of steel. Corrosion potential area ( $E_{\text{corr}}$ ) indicates potential area of corrosion which causes corrosion. After that,  $E_{\text{cor}}$ ,  $E_{\text{passive}}$ , dan  $E_{\text{transpassive}}$  points were followed by the manufacture of E-pH diagram of a collection of these points. This was done in a solution without and with the inhibitor.

### 3. Results and discussion

E-pH diagram 304SS was constructed by potentiodynamic method.



**Figure 2:** Typical polarization curves of 304SS in pH 0 solution without inhibitor (a), with BWP extract inhibitor 2000ppm (b)

Based on polarization curves the value of  $E_{\text{corr}}$ ,  $i_{\text{corr}}$ ,  $E_{\text{passive}}$ , dan  $i_{\text{passive}}$  at each pH was determined.  $E_{\text{corr}}$  indicates pH potential area which causes metal corrosion with increasing potential value towards the positive. In determining  $E_{\text{passive}}$ , the corrosion rate looks as if it stopped and the anodic current density did not increase with the increase in the potential. The passive layer is a corrosion product and this layer protects the metal underneath as it becomes a barrier that prevents the corrosive environment in contact with the metal under the passive layer. Based on this, the solution E-pH diagram without inhibitor and with the inhibitor of BWP extract was made (Figures 3 and 4).

The result obtained from polarization of pH 0-14 in solution without BWP extract inhibitor is seen in the E-pH diagram of Figure 3. At pH 0-7 an active immune border occurred at a potential below 0 (negative). Corrosion potential increased at 8-10, decreased at pH 11, increased at pH 12 and decreased again at pH 13. The same pattern occurred at the boundary between the active and passive area shown on  $E_{\text{passive}}$  at all pH. Passive area at pH 8-11 is larger than that at pH 0-7 since  $E_{\text{transpassive}}$  value increases at pH 8-12. The active area is greater at an acidic pH compared to alkaline and neutral pH. This is due to acidic condition in the solution which determines the pH where the corrosion rate increases rapidly along with the hydrogen evolution reaction [20].

Based on the construction of E-pH diagram with the addition of 2000 ppm in figure 4, it is known that the diagram has the same pattern with the E-pH diagram without inhibitor. Passive area appears to be larger at pH above 6. Compared to the E-pH diagram without inhibitor, image 5.8 showed larger passive area at pH above 6. A striking difference occurred once at pH 13 in passive area.

The extent of active, passive and immune areas was calculated by the Finite Element Method (FEM) with the method of determining the extent of the coordinate point. Immune area declared sectional area I, an active area declared sectional area II and passive area declared sectional area III. Based on the result of the calculation, the extent of immune, active and passive areas on the E-pH diagram with the addition of inhibitor is 15.1813; 9.03842; 17.779. It seems that the active area with the addition of inhibitor is smaller than is without inhibitor.

In contrast, the passive area without the addition of inhibitor is greater than is with the addition of inhibitor. Shrinkage in the addition of inhibitors amounted to 15.697% and passive area magnification is of 6.01%. This shows that the inhibition mechanism is by adsorption on polarization [9]. As a result, it appears that the BWP extract is a mixed type that mostly towards the anodic polarization which means oxidation reaction is inhibited more in the adsorption process with the inhibitor.

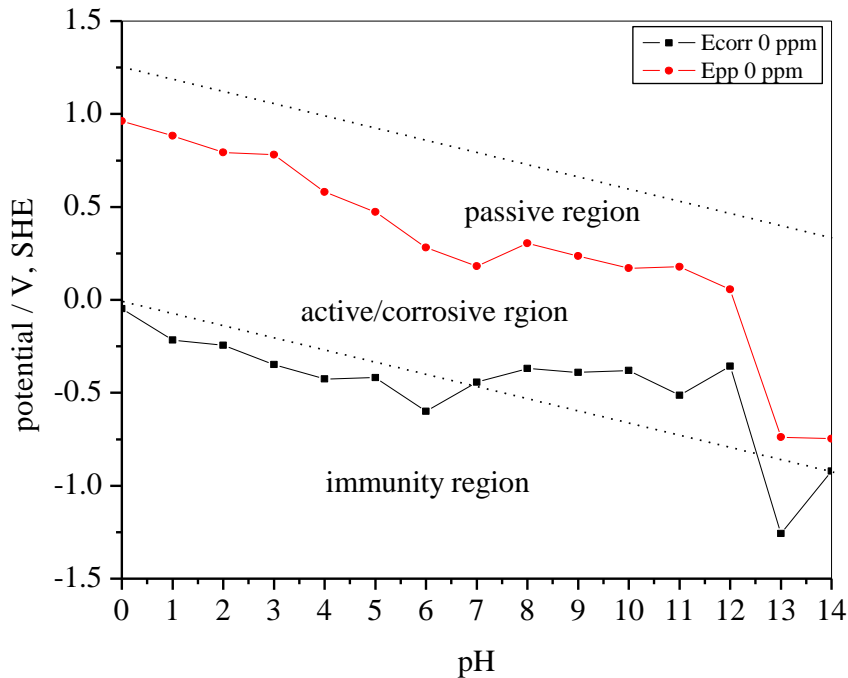


**Figure 3:** E-pH diagram in solution without BWP extract inhibitor in  $H_2SO_4$  system

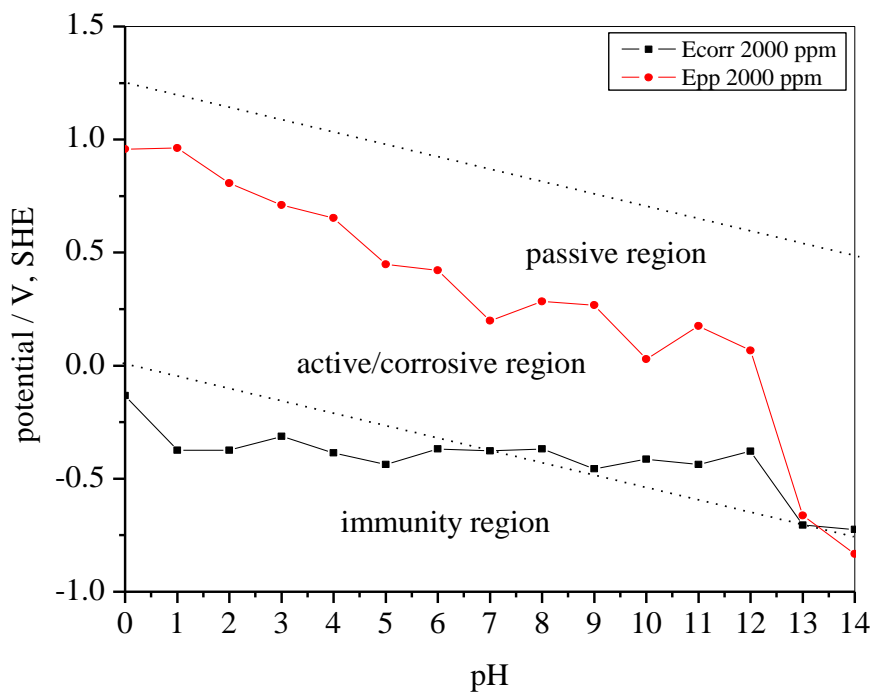


**Figure 4:** E-pH diagram in solution with BWP extract inhibitor in  $H_2SO_4$  system

On more positive potentials, the corrosion rate increased and reached the maximum of the passivation potential. Passivation can be defined as the loss of the chemical reactivity of metal under a certain environmental condition, due to the formation of a protective membrane [21]. Increasingly large passive areas result from the

potential on the line Epp is lower so that Ecorr-Epp difference is smaller. This narrows the area of corrosion as pitting corrosion on the specimen does not occur [22]. It proves the specimen surface is finer since there is protection on metals and no corrosion trigger. Large passive area is due to their protection of BWP extract inhibitor [23]. For that needs, testing the AFM in the area should be conducted. Larger passive area is due to the mechanism of inhibition conducted by BWP extract in the form of adsorption. Sampling is performed at pH 13 which shows the difference between the E-pH diagram without and with inhibitor.

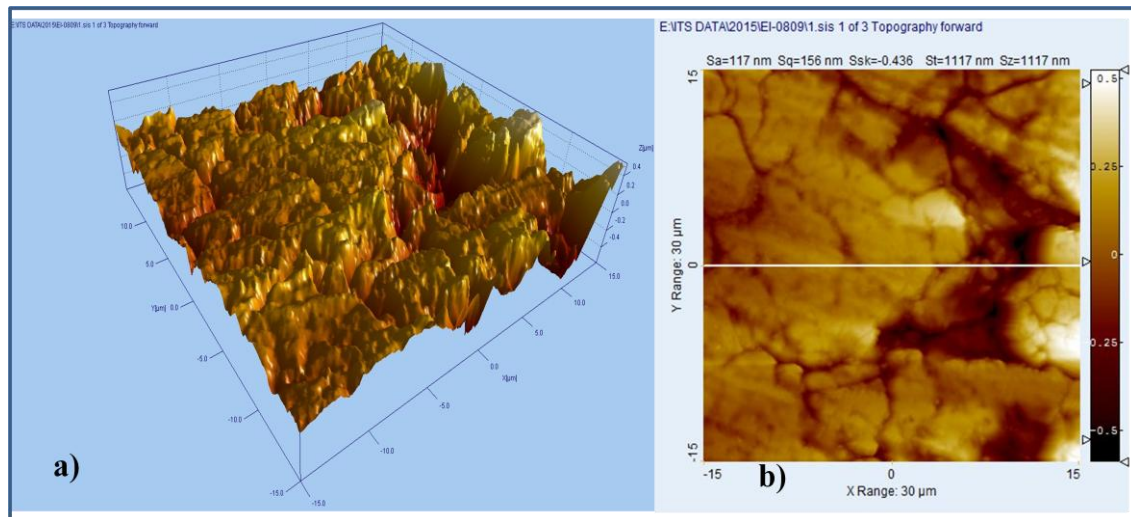


**Figure 5:** 3-D topography (a), 2-D topography of SS 304 surface in pH 13 without BWP extract inhibitor (b).

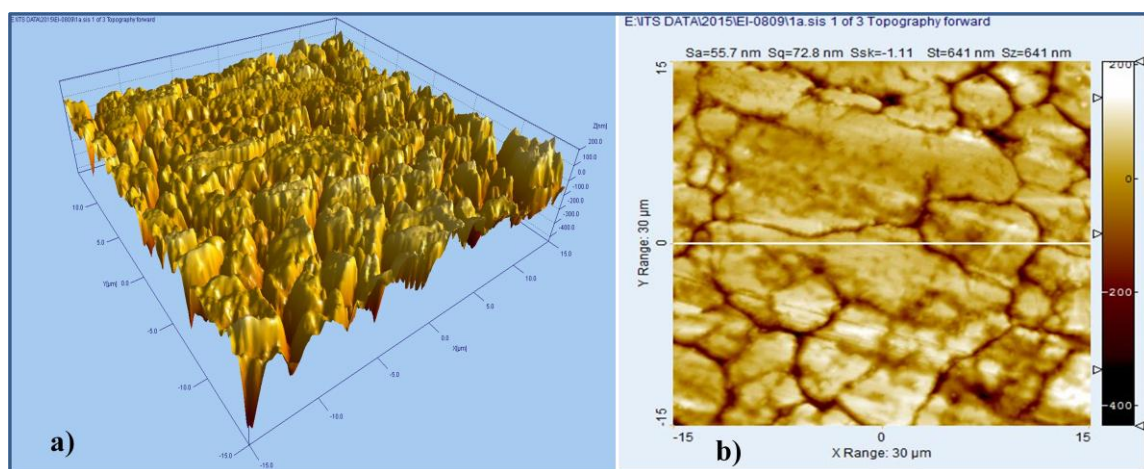


**Figure 6:** 3-D topography (a), 2-D topography of SS 304 surface in pH 13 with BWP extract inhibitor (b).

At pH 13 it shows that passive area indicated greater possibility of passive layer on the specimen. Figure 5 is a picture of the topography of the 3-D and 2-D surface of SS 304 at pH 13 with BWP extract inhibitor. AFM is a technique that is appropriate to analyze the morphology of the metal surfaces influenced by the inhibitor on the interface of a metal or a solution [24-27]. Figure 5 shows SS304 surface without the addition of inhibitor after in a solution of pH 13, the surface structure of 304SS has large and deep pores. In addition, it looks more coarse with an average surface of 1117 nm. Yet the surface is much smoother at 641 nm which is the metal surface by the addition of BWP extract inhibitor in solution pH 13 (Figure 6). Inhibitor molecules are adsorbed on the surface of the steel and are protected by SS 304 metal against corrosion. The result showed that the passive layer looks more numerous in pH by the addition of BWP extract inhibitor in the solution of pH 13. The test results confirm the AFM passive layer resulting from the addition of inhibitor to the solution.

## Conclusion

Passive area is increasingly larger marked with the decreasing passive potential value at each pH, in which the potential value is lower than aqueous solutions of water oxidation. Low potential value will narrow the active or corrosion area due to the small difference of  $E_{\text{corr}}-E_{\text{passive}}$ . Active area on the E-pH diagram with inhibitor decreases of 15.69% and a passive area enlarges 6.01 BWP % . The BWP inhibitor extract provides protection against 304SS steel through the mechanism of adsorption. At the same time, it forms a passive layer on the surface as well.

## References

1. Benabdellah M., Benkaddour M., Hammouti B., Bendahhou M., Aouniti A., *App. Surf. Sci.* 252 (2006) 6212.
2. Ahmad Z., Elsevier. Oxford. (2006).9780080480336.
3. Abdallah.,M., *Corros. Sci.* 44 (2002) 717.
4. Fouda A.S., Mostafa H.A., El-Abbasy H.M., *J. Appl. Electrochem.* 40 (2010) 163
5. Fouda A.S., Elewady G.Y., El-Haddad M. N., *Canadian J. Sci. & Ind. Res.* 2 (2011) 1.
6. Oguzie E. E., Unaegbu C., Ogukwe C. N., Okolue B. N., Onuchukwu A. I., *Mater. Chem. Phys.* 84 (2004) 363.
7. Quraishi M.A., Singh A., Yadav D. K., Singh A.K., *Mater. Chem. Phys.* 122 (2010) 114.
8. El-Etre A.Y., *Corros. Sci.* 45 (2003) 2485.
9. Gapsari F., Soenoko R., Suprpto A., Suprpto W., *Int. J. Corros. I* (2015).
10. Abdallah M., *Mater. Chem. Phys.* 82 (2003) 786.
11. Pourbaix M. Staehle R.W., *Lectures on Electrochemical Corrosion* Ed. Springer US, (1973), ISBN: 978-1-4684-1804-4.
12. Pourbaix., *Atlas of Electrochemical Equilibria in Aqueous Solutions* (1974).9780915567980.
13. Cramer, Covino., *ASM Handbook*, 13A (2003).978-0-87170-705-5.
14. Kelly R.G., Scully J.R., Shoesmith D. W., Buchheit R.G., *Electrochemical Techniques in Corrosion Science and Engineering* (2002). 0-8247-9917-8.
15. Pourbaix M., *Atlas of Electrochemical Equilibria in Aqueous Solutions* (1966).
16. Fontana M.G., *Corrosion Engineering.* (1987). 0070214638.
17. Jones D.A., *Principles and Prevention of Corrosion* (1985). 0133599930.
18. Stansbury E.E., Buchanan R.A., *Fundamentals of Electrochemical Corrosion* (2000).1615030670.
19. ASTM G1-72., *Practice for Preparing, Cleaning and Evaluating Corrosion Test Specimens;* ASTM, (1990).
20. Uhlig, *Uhlig's Corrosion Handbook* (2011).978-0-470-08032-0.
21. Lothongkum G., Vongbandit P., Nongluck P., *Anti-Corros. Meth. Mater.* 53 (2006) 169.
22. Baboian R, *Galvanic and Pitting Corrosion-Field and Laboratory Studies;* ASTM (1974). 04-576000-27.
23. Sastri V.S., *Corrosion Inhibitors Principles and Applications* (1998). 0471976083.
24. D'oner A., Solmaz R., Ozcan M., Kardas G., *Corros. Sci.* 53 (2011) 2902.
25. Umoren S.A., Li Y., Wang F.H., *Corros. Sci.* 52 (2010) 1777.
26. Wang B., Du M., Zhang J., Gao G.J., *Corros. Sci.* 53 (2011) 353.
27. Solmaz R., Kardas G., Culha M., Yazıcı B., Erbil M., *Electrochim. Acta* 53 (2008) 5941.

(2016) ; <http://www.jmaterenvironsci.com/>